Crystal Size Distribution patterns for lunar meteorites Northwest Africa 12008, 4898, 8632, 3136 and three LaPaz Icefield lunar meteorites. Stu Webb[1], C. R. Neal[1], A. Gawronska[2], and J.M.D. Day[3] [1]Department of Civil and Environmental Engineering and Earth Science, University of Notre Dame, Notre Dame, IN 46556, USA [gwebb1@nd.edu; cneal@nd.edu]. [2]Dept. of Geology & Env. Earth Science, Miami University of Ohio, Oxford, ON45056. [3]Scripps Institution of Oceanography, University of California San Diego, La Jolla CA 92093-0244, USA.

Introduction: Crystal Size Distribution (CSD) data are a valuable tool for evaluating the crystallization histories of both lunar and terrestrial igneous samples [1-3]. For lunar basalts, CSDs have also been proposed as a quantitative method to differentiate between impact melts and basalts produced by partial melting of the lunar mantle (endogenic processes) [4]. Plotting CSD slope and y-intercept data for lunar meteorite samples can help identify potentially-related lunar meteorite samples, and it may also help provide constraints on whether some of the basaltic lunar meteorites represent impact melts.

While some work on lunar meteorite CSDs has already been done [5,6], this study presents data for lunar meteorite thin sections whose CSDs have not been previously reported. While prior work has been performed on LaPaz Icefield samples 02205, 02224, and 02226 [5], NWA 032 [5], and NWA 8632 [6], this study reports new data from thin sections of those samples that have not previously been texturally analyzed using this method as well as for basaltic lunar meteorites NWA 12008 [7], NWA 4898, NWA 4734, and basaltic clasts within the polymict breccia lunar meteorite NWA 3136. Olivine CSDs were constructed for basaltic lunar meteorites NWA 8632 and NWA 032, while plagioclase CSDs were constructed for the other meteorites in this study. The CSDs from these samples may be plotted with those previously reported from other lunar basalts (e.g., [4]) and used to create a basis for comparison and classification.

Methods: CSD data for this study was collected in a manner similar to that listed in [4], but with slight variations. Photomicrographs of the thin sections were obtained using a Nikon petrographic microscope in plane-polarized light, cross-polarized light, and reflected light. A 4× objective was used for all images. Once the images were collected they were then stitched together using Microsoft *Image Composite Editor*© to create a photomosaic representing the entirety of the sample. These stitched photomosaics were then opened in Corel *Paintshop*© *Pro 2019 Ultimate* on a touchscreen 2-in-1 laptop computer and the plagioclase or olivine crystals were traced using an active stylus. In NWA 12008 and NWA 4898 the plagioclase crystals had been converted to maskelynite, so the maskelynite areas were traced in lieu of tracing plagioclase crystals. In the case of intersecting crystals multiple layers were generated in *Paintshop*© *Pro* to ensure that each crystal was recorded discretely and that no crystals were merged together while tracing. 250 crystals are considered the minimum number necessary for the CSD to be considered statistically viable [2], but care was taken to trace the absolute maximum number of crystals available in each sample area in order to achieve population density values that are as accurate as possible. Once the crystal traces were completed the photomosaics were removed from the background and the crystal traces were filled-in with a solid color. Those images were exported to *ImageJ*©, where the known scale of the images was used to determine the area, best-fit ellipse, and major/minor axis of each crystal and the sample area itself. This data was then input into *CSDSlice* [2] and *CSDCorrections* [3] to determine the overall shape and size distribution of the crystals. *CSDCorrections* measurement options were set to Ellipse Major Axis and the size scale was five bins per decade. The resulting *CSDCorrections* data was used to plot the natural log (ln) of population density versus the length of each crystal's major axis (Fig. 1).

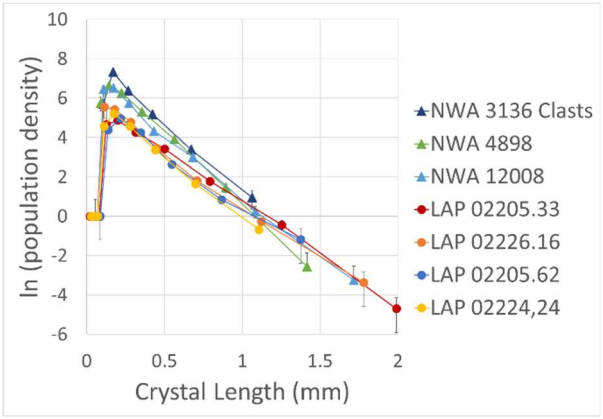

Figure 1: Plagioclase CSD profiles for LAP 02205,62, LAP 02226,16, LAP 02205,33, LAP 02224,24, NWA 3136 basalt clasts, and maskelynite CSD profiles for NWA 12008 and NWA 4898 to represent plagioclase distribution. If error bars are not visible then they are within the size of the symbol.

Results and Discussion: All four of the paired LaPaz Icefield samples had similar CSD slopes and y-intercepts, with the data similar to that measured by Day and Taylor [5]. NWA 12008 displayed a similar CSD slope but a higher y-intercept, indicating a greater population density of plagioclase crystals than was measured in the

LaPaz samples. NWA 4898 displays a higher y-intercept and steeper slope than the NWA 12008 CSD, while the plagioclase CSDs from the basalt clasts in NWA 3136 are similar to NWA 4898 but have the steepest slope and highest population density of any plagioclase CSD in this study. The NWA 8632 and NWA 032 olivine CSDs plot closely to one another and both are within the endogenous field as opposed to the impact melt region. Both NWA 8632 and NWA 032 olivine CSDs show a steeper slope and higher y-intercept than have previously been reported in other thin sections from these meteorites [5,6]. None of the samples fall into the currently proposed field for impact melts when plotted on a y-intercept versus CSD slope graph (Fig. 2, Fig. 3).

These data can be compared to other lunar basalts collected during the Apollo program. All basaltic lunar meteorites are of the low-Ti variety and the CSDs plot with the Apollo 12 or Apollo 14 basalts in Figures 2 and 3. NWA 12008 plots to the left of the Apollo 12 low-Ti basalts. Further investigations will be required to determine if this sample represents a new low-Ti mare basalt variety.

Conclusions: Plagioclase CSDs from these lunar meteorites indicate they are endogenous melts from the lunar mantle rather than impact melts (Fig. 3), providing evidence for possible relationships between different lunar meteorites or between these meteorites and samples collected on the surface of the moon. Further textural studies of additional lunar meteorites will provide a more robust database. The CSDs of the low-Ti basaltic lunar meteorites are similar to those from Apollo 12 and 14 basalts (Fig. 3), although NWA 12008 does not fall within these fields. Further work is necessary to evaluate if it represents a new variety of low-Ti mare basalt.

References: [1] Marsh, B. D. (1988) *Contributions to Mineralogy and Petrology 99*, 277–291. [2] Morgan D. J., & Jerram D.A. (2006) *JVGR 154*, 1-7. [3] Higgins M.D. (2000) *Amer. Min. 85*, 1105-1116. [4] Neal C. R. et al. (2015) *GCA 148*, 62-80. [5] Day J. M. D., & Taylor L. A. (2007) *Meteoritics & Planetary Science 42*, Nr 1, 3–17. [6] Cato M. J., Fagan A. L., & Gross, J. (2016) LPSC 47 [7] Cohen M.E. et al. (2019) LPSC 50

Acknowledgement: We thank Tony Irving, University of Washington, for allowing us access to the thin sections of many of the lunar meteorites, especially the newly discovered NWA 12008.

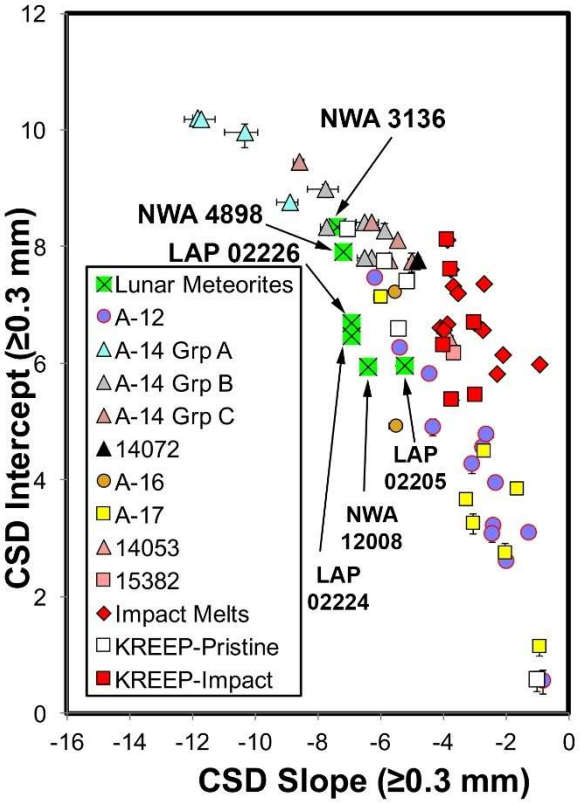

Figure 2: Meteorite samples from this study compared with plagioclase CSDs from other lunar basalts and impact melts [4].

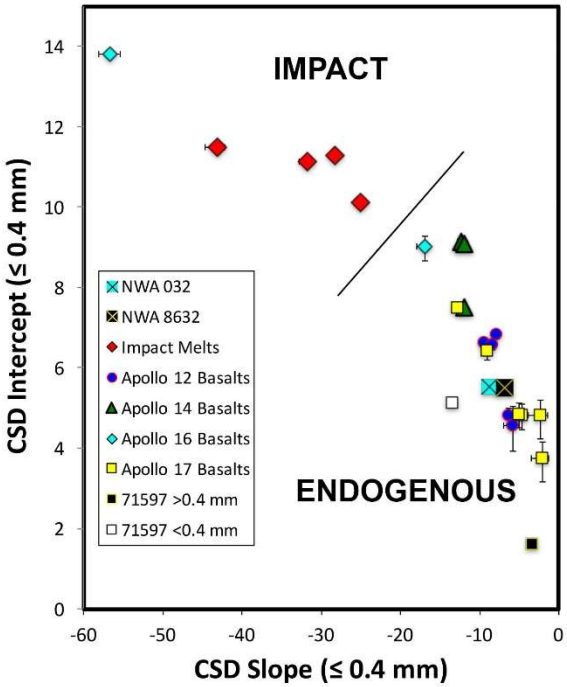

Figure 3: Meteorite samples from this study compared with olivine CSDs from other lunar basalts and impact melts [4].